AIAA JOURNAL
Vol. 35, No. 2, February 1997

# Method for Structural Model Update Using Dynamically Measured Static Flexibility Matrices

Keith K. Denoyer*
*U.S. Air Force Phillips Laboratory, Kirtland Air Force Base, New Mexico 87117-5776*
and
Lee D. Peterson†
*University of Colorado, Boulder, Colorado 80309-0429*

**A new method is presented for parametric correction of full-order analytical stiffness matrices from reduced-order dynamically measured static flexibility matrices. The measured static flexibility matrix is formed using modal data in conjunction with a residual flexibility estimate. The algorithm corrects model parameters by minimizing a static flexibility matrix error residual constructed for measurement degrees of freedom only. By utilizing a flexibility matrix residual instead of one derived using stiffness matrices, numerical problems associated with inverting a rank-deficient measured flexibility matrix are avoided. Posing the problem in terms of flexibility matrices also avoids the problems of modal correspondence, mode selection, and modal truncation. In addition, incorporating static reduction relationships into the error residual makes prior eigenvector expansion or model reduction unnecessary. Two formulations for the error residual are presented: an explicit inverse formulation and one derived from a pseudoinverse relationship. The second leads to an exact linear update problem when all of the model degrees of freedom are measured. Numerical simulation results demonstrate that both formulations are capable of localizing and quantifying local stiffness errors in a full-order finite element model from reduced-order measurements. Experimental results for a cantilever beam structure are also presented.**

## Introduction

THE ability to localize and quantify modeling errors or structural damage is becoming an increasingly important factor in maintaining performance, reliability, and cost effectiveness in a wide variety of applications. These applications include aircraft and spacecraft, various types of mechanical machinery, and civil structures such as buildings, bridges, and offshore oil/gas platforms.

The most common approach to the model update problem has been to seek a refined finite element model whose modal properties are in agreement with those from an experimental modal analysis of the structure. A considerable amount of work in this area has been published. Most of this research has centered on three model update approaches: optimal matrix update, sensitivity-based parameter update, and eigenstructure assignment. A good introductory overview of these techniques may be found in Ref. 1.

An advantage of modal-based update methods is that they utilize data obtained from established modal testing techniques. These techniques have been successfully applied to model reconciliation and damage detection problems for a variety of structures. However, several difficulties remain that make modal-based techniques impractical in many instances. For a modally complex structure, it is often difficult to determine the correspondence between experimental modes and modes from the analytical model. To achieve good performance from techniques that minimize differences between experimental and analytical mode shapes and frequencies, determining modal correspondence is crucial. Another problem is choosing an appropriate set of modes to use for the update. For computational reasons, it is desirable to use as few modes as possible because most modal-based update methods require computationally expensive nonlinear optimizations. However, modes must be included that are sensitive to the local model errors that the algorithm is trying to localize. This suggests using as many modes as possible. In practice, a compromise between these conflicting requirements must be made. A third problem is modal truncation due to a finite measurement bandwidth. Because the effects of residual dynamics from modes outside the measurement bandwidth are neglected, the measurements can only provide incomplete information about the structure.

One way to avoid these problems is to use measured static data in the update process rather than modal data. Several update techniques have been developed along these lines and include those proposed by Lallement et al.,[2] Hajela and Soeiro,[3] and Sanayei and Onipede.[4] Typically, these are sensitivity-based algorithms that perform an update using deflection shapes obtained from static testing. However, static testing has some serious drawbacks, including an inability to handle free-free boundary conditions, additional cost associated with instrumentation and construction of stiff support fixtures, and potential dangers to the test article from relatively high load levels.

An alternative to using measured static deflection data is to use a measured static flexibility matrix obtained from dynamic test data. Recently developed techniques for fitting experimental data for complex structures have led to a computationally practical approach for obtaining estimates of normal modes and residual flexibility, which are then used to form a measured static flexibility matrix.[5–9] In this paper, a new model update approach is presented that utilizes dynamically measured static flexibility matrices and avoids many of the problems encountered using modal-based techniques or techniques that use measured static deflection data.

This new approach also addresses another major obstacle in the model update problem: the problem of a reduced number of measurement degrees-of-freedom (DOF). In a typical problem, the model has many more DOF than the measurements. This implies that the measurements must be expanded or the model must be reduced before a comparison of the two can be made. This is usually accomplished through eigenvector expansion or a model reduction technique such as Guyan reduction.[10] Problems are often encountered due to errors introduced by the expansion process and from the smearing effect on modeling errors introduced by model reduction, making error localization difficult. The new approach addresses this problem by incorporating the relationship between measurement and model DOF directly into the flexibility error equation used to perform the parameter correction. This allows the full-order model

Presented as Paper 96-1281 at the Dynamic Specialist Conference, Salt Lake City, UT, April 18, 1996; received June 3, 1996; revision received Oct. 23, 1996; accepted for publication Oct. 24, 1996; also published in *AIAA Journal on Disc*, Volume 2, Number 2. 

*Research Engineer, Space Technology Directorate, Space Vehicle Technologies Division. Member AIAA.

†Associate Professor, Center for Aerospace Structures and Department of Aerospace Engineering Sciences. Senior Member AIAA.

to be updated with a reduced-order measured flexibility matrix. In addition, using a flexibility rather than a stiffness matrix residual avoids numerical difficulties associated with inverting a reduced-rank measured flexibility matrix. The measured flexibility matrix is typically rank deficient because only incomplete modal information and a partial estimate of the residual flexibility are usually available.

The remainder of this paper presents the theoretical development of the flexibility-based update approach as well as numerical simulation results for the simple eight DOF discrete model introduced by Kabe.[11] In addition, experimental results are presented for a cantilever beam structure.

## Theoretical Development

### Static Finite Element Model Update Problem

Assume we are given a static finite element model of the form

$$\tilde{K}\{q\} = \{f\} \tag{1}$$

where $\tilde{K}$ is the structural stiffness matrix of the nominal analytical model in global coordinates, $\{q\}$ is a set of generalized coordinates corresponding to the $n$ global DOF, and $\{f\}$ is the set of generalized nodal forces. The problem is to find a perturbation matrix $\Delta K$ that can be used to update $\tilde{K}$ so that the model correlates with available experimental data. In other words, a new model is sought such that

$$K\{q\} = \{f\} \tag{2}$$

where the updated analytical stiffness matrix $K$ is given by

$$K = \tilde{K} + \Delta K \tag{3}$$

It is also desired that this new model retain the basic properties of the original model such as symmetry, positive definiteness, and model connectivity.

### Parametrization of the Stiffness Matrix

Many possibilities exist for parametrization of the analytical stiffness matrix. A general approach is to write the stiffness matrix perturbation as a linear combination of sensitivity matrices such that

$$\Delta K = \sum_{i=1}^{n_P} \alpha_i S_i \tag{4}$$

where $n_P$ is the number of parameters being updated and the $S_i$ are the normalized sensitivity matrices given by

$$S_i = \tilde{p}_i \frac{\partial K}{\partial p_i} \tag{5}$$

where $\tilde{p}_i$ is the nominal value of the $i$th parameter. The $\alpha_i$ are simply the normalized changes to the updated parameter $p_i$ given by the following ratio:

$$\alpha_i = \frac{p_i - \tilde{p}_i}{\tilde{p}_i} \tag{6}$$

In other words, the $\alpha_i$ indicate the percentage change of parameter $p_i$ from the nominal model. Note that Eq. (4) is consistent with the submatrix scaling parametrization proposed by Lim.[12] As a practical matter, approximations to the $S_i$ matrices in this formulation are easily obtained from commercial finite element codes by varying the corresponding parameter and observing the net change to the global stiffness matrix. This is particularly useful when the exact element formulation is unavailable.

### Flexibility Error Equation

The goal of the present model update procedure is to determine the $\alpha_i$ of Eq. (6) that minimize the error between the measured and analytical static flexibility matrices. This problem can be expressed as

$$\min_{\alpha} \left\| G^M - G_{mm} \right\| \tag{7}$$

where $G^M$ is the measured flexibility matrix obtained at the measurement DOF, which are typically a small subset of the analytical DOF. Similarly, $G_{mm}$ is the partition of the analytical flexibility matrix corresponding to the measured DOF only. Equation (7) forms the basis for a flexibility-based model update approach. However, several specific issues need to be resolved before implementation is possible. Two of these are the formation of $G_{mm}$ and the choice of a solution method for Eq. (7). In the sections that follow, two approaches for the formation of $G_{mm}$ are presented: an explicit inverse formulation that uses a static reduction of the analytical stiffness matrix to form $G_{mm}$ and an approximation to $G_{mm}$ based on a pseudoinverse relationship. Linear and nonlinear solutions are developed for both approaches.

### Explicit Inverse Formulation of Analytical Flexibility Matrix

The static flexibility matrix is defined as the inverse of the structural stiffness matrix,

$$G \equiv K^{-1} \tag{8}$$

Partitioning the matrices into measurement DOF and omitted DOF not contained in the measurement, Eq. (8) becomes

$$\begin{bmatrix} G_{mm} & G_{mo} \\ G_{mo}^T & G_{oo} \end{bmatrix} = \begin{bmatrix} K_{mm} & K_{mo} \\ K_{mo}^T & K_{oo} \end{bmatrix}^{-1} \tag{9}$$

Utilizing an expression for the inverse of a block matrix,[13] the upper left partition of Eq. (9) becomes

$$G_{mm} = \bar{K}^{-1} \tag{10}$$

where $\bar{K} = K_{mm} - K_{mo} K_{oo}^{-1} K_{mo}^T$ is simply the static or Guyan[10] reduction of the analytical stiffness matrix onto the measurement DOF. Using Eq. (10), Eq. (7) can now be written

$$\min_{\alpha} \|F(\alpha)\| \tag{11}$$

where

$$F(\alpha) \equiv G^M - \left(K_{mm} - K_{mo} K_{oo}^{-1} K_{mo}^T\right)^{-1} \tag{12}$$

Expanding $F(\alpha)$ in terms of the perturbation to the original model, we get

$$F(\alpha) = G^M - \big[\tilde{K}_{mm} + \Delta K_{mm} - (\tilde{K}_{mo} + \Delta K_{mo}) \times (\tilde{K}_{oo} + \Delta K_{oo})^{-1} (\tilde{K}_{mo}^T + \Delta K_{mo}^T)\big]^{-1} \tag{13}$$

An examination of Eq. (4) shows that Eq. (13) is nonlinear with respect to the unknown $\alpha_i$. To solve the minimization problem, either a linear approximation must be used or an iterative nonlinear approach employed.

In the remainder of the paper, the algorithm that performs a parameter correction based on minimizing Eq. (13) will be referred to as the flexibility error reduction algorithm (FLEX).

### Approximate Linear Least-Squares Solution

To obtain a linear solution, $F(\alpha)$ is rewritten in terms of its Taylor series expansion about $\alpha = 0$ as

$$F(\alpha) = F(0) + \sum_{i=1}^{n_P} \frac{\partial F}{\partial \alpha_i}\bigg|_{\alpha=0} \alpha_i + N(\alpha) \tag{14}$$

The first term $F(0)$ is obtained by setting the $\alpha_i = 0$ in Eq. (13), which gives

$$F(0) = G^M - \left(\tilde{K}_{mm} - \tilde{K}_{mo} \tilde{K}_{oo}^{-1} \tilde{K}_{mo}^T\right)^{-1} \tag{15}$$

which is simply the flexibility error for the nominal model at the measurement DOF. In Layton,[14] it is shown that the partial derivative of the matrix inverse may be written as

$$\frac{\partial A^{-1}}{\partial \alpha_i} = -A^{-1} \frac{\partial A}{\partial \alpha_i} A^{-1} \tag{16}$$

Using this relationship as well as the sensitivity expressions given in Eq. (4), the $i$th derivative term may be expressed as

$$\frac{\partial F}{\partial \alpha_i} = \bar{K}^{-1}\left(S_{i_{mm}} - S_{i_{mo}} K_{oo}^{-1} K_{mo}^T - K_{mo} K_{oo}^{-1} S_{i_{mo}}^T + K_{mo} K_{oo}^{-1} S_{i_{oo}} K_{oo}^{-1} K_{mo}^T\right)\bar{K}^{-1} \tag{17}$$

where again $\bar{K} = K_{mm} - K_{mo} K_{oo}^{-1} K_{mo}^T$ and the subscripts $mm$, $mo$, and $oo$ correspond to measured and omitted DOF partitions of the respective matrices. Evaluating this expression when $\alpha_i = 0$, Eq. (17) becomes

$$\left.\frac{\partial F}{\partial \alpha_i}\right|_{\alpha=0} = \bar{K}_{\text{nom}}^{-1}\left(S_{i_{mm}} - S_{i_{mo}} \tilde{K}_{oo}^{-1} \tilde{K}_{mo}^T - \tilde{K}_{mo} \tilde{K}_{oo}^{-1} S_{i_{mo}}^T + \tilde{K}_{mo} \tilde{K}_{oo}^{-1} S_{i_{oo}} \tilde{K}_{oo}^{-1} \tilde{K}_{mo}^T\right)\bar{K}_{\text{nom}}^{-1} \tag{18}$$

where $\bar{K}_{\text{nom}} = \tilde{K}_{mm} - \tilde{K}_{mo}\tilde{K}_{oo}^{-1}\tilde{K}_{mo}^T$ is the static reduction of the nominal analytical stiffness matrix. If we neglect any higher-order and nonlinear terms contained in $N(\alpha)$, a linear matrix equation can be written for $\alpha_i$ as

$$\sum_{i=1}^{np} C_i \alpha_i = F(0) \tag{19}$$

where the constant matrix $C_i$ is given by

$$C_i = -\left.\frac{\partial F}{\partial \alpha_i}\right|_{\alpha=0} \tag{20}$$

Because the matrices involved are symmetric, the unique entries can be used to write the problem in the familiar linear least-squares form as

$$C\{\alpha\} = \{B\} \tag{21}$$

where the $i$th column of $C$ is formed from the unique entries of $C_i$ and the vector $\{B\}$ is formed from the unique entries of the matrix $B$. In general, $N(\alpha)$ will be nonzero for this approach. Therefore, the linear solution will generally be only used as a starting point for a nonlinear iterative solution algorithm.

### Nonlinear Solution

Many techniques exist for the minimization of nonlinear functions. The results that follow use the Davidon–Fletcher–Powell metric gradient search method.[15] Because use of the Froebenius norm facilitates calculation of the gradient needed for this technique, it is used in Eq. (11) and the function to be minimized becomes

$$\|F(\alpha)\|_F^2 = \sum_{j=1}^{m}\sum_{k=1}^{m}[F_{jk}(\alpha)]^2 \tag{22}$$

where $m$ is the number of measurement DOF. To avoid numerical conditioning problems, this function is normalized by the function value at the initial parameter estimate to give the following objective function:

$$J = \frac{\|F(\alpha)\|_F^2}{\|F(\alpha_0)\|_F^2} \tag{23}$$

The gradient is then found by taking the derivatives of $J$ with respect to $\alpha_i$, which are given by

$$\frac{\partial J}{\partial \alpha_i} = \frac{1}{\|F(\alpha_0)\|_F^2}\sum_{j=1}^{m}\sum_{k=1}^{m} 2F_{jk}(\alpha)\left[\frac{\partial}{\partial \alpha_i}F(\alpha)\right]_{jk} \tag{24}$$

where $(\partial/\partial\alpha_i)F(\alpha)$ is given by Eq. (17).

### Approximate Pseudoinverse Formulation for the Analytical Flexibility Matrix

One of the drawbacks of explicitly forming $G_{mm}$ is the need to calculate $\bar{K}^{-1}$. Another approach is to define the structural flexibility as the Moore–Penrose pseudoinverse[16] of the structural stiffness matrix:

$$G \equiv K^{+} \tag{25}$$

From the definition of the Moore–Penrose pseudoinverse, we can write

$$G = GKG \tag{26}$$

Expanding Eq. (26) for the $G_{mm}$ partition yields

$$G_{mm} - G_{mm}K_{mm}G_{mm} - G_{mo}K_{mo}^T G_{mm} - G_{mm}K_{mo}G_{mo}^T - G_{mo}K_{oo}G_{mo}^T = 0 \tag{27}$$

As before, $G_{mo}$ is related to $G_{mm}$ by

$$G_{mo} = -G_{mm}K_{mo}K_{oo}^{-1} \tag{28}$$

and Eq. (27) reduces to

$$G_{mm} = G_{mm}K_{mm}G_{mm} - G_{mm}K_{mo}K_{oo}^{-1}K_{mo}^T G_{mm} \tag{29}$$

One way to avoid explicitly forming an inverse to get $G_{mm}$ is to substitute the measured flexibility matrix $G^M$ for $G_{mm}$ in the right-hand side of Eq. (29). This leads to the estimate $\hat{G}_{mm}$ given by

$$\hat{G}_{mm} = G^M K_{mm} G^M - G^M K_{mo} K_{oo}^{-1} K_{mo}^T G^M \tag{30}$$

The justification for making this substitution lies with the fact that in the limit that $\hat{G}_{mm}$ approaches $G^M$, $G_{mm}$ will also approach $G^M$. Therefore, substituting $\hat{G}_{mm}$ for $G_{mm}$ in Eq. (7) is acceptable as long as the final error residual is small. Following the development of the earlier approach, $F(\alpha)$ can now be written

$$F(\alpha) = G^M - G^M K_{mm} G^M + G^M K_{mo} K_{oo}^{-1} K_{mo}^T G^M \tag{31}$$

and

$$F(0) = G^M - G^M \tilde{K}_{mm} G^M + G^M \tilde{K}_{mo} \tilde{K}_{oo}^{-1} \tilde{K}_{mo}^T G^M \tag{32}$$

$$\frac{\partial F}{\partial \alpha_i} = -G^M\left(S_{i_{mm}} - S_{i_{mo}} K_{oo}^{-1} K_{mo}^T - K_{mo} K_{oo}^{-1} S_{i_{mo}}^T + K_{mo} K_{oo}^{-1} S_{i_{oo}} K_{oo}^{-1} K_{mo}^T\right)G^M \tag{33}$$

$$\left.\frac{\partial F}{\partial \alpha_i}\right|_{\alpha=0} = -G^M\left(S_{i_{mm}} - S_{i_{mo}} \tilde{K}_{oo}^{-1} \tilde{K}_{mo}^T - \tilde{K}_{mo} \tilde{K}_{oo}^{-1} S_{i_{mo}}^T + \tilde{K}_{mo} \tilde{K}_{oo}^{-1} S_{i_{oo}} \tilde{K}_{oo}^{-1} \tilde{K}_{mo}^T\right)G^M \tag{34}$$

Using Eqs. (32) and (34), the nonlinear remainder term of Eq. (14) can be expressed as

$$N(\alpha) = G^M\left[\tilde{K}_{mo}\tilde{K}_{oo}^{-1}\Delta K_{oo}\tilde{K}_{oo}^{-1}\tilde{K}_{mo}^T + \Delta K_{mo}\tilde{K}_{oo}^{-1}\Delta K_{mo}^T - \tilde{K}_{mo}\kappa\tilde{K}_{mo}^T - \tilde{K}_{mo}\kappa\Delta K_{mo}^T - \Delta K_{mo}\kappa\tilde{K}_{mo}^T - \Delta K_{mo}\kappa\Delta K_{mo}^T\right]G^M \tag{35}$$

where $\kappa = \tilde{K}_{oo}^{-1}(\tilde{K}_{oo}^{-1} + \Delta K_{oo}^{-1})^{-1}\tilde{K}_{oo}^{-1}$. It is interesting that when all of the model error is contained in elements that only touch measurement DOF, $\Delta K_{oo} = 0$ and $\Delta K_{mo} = 0$. Also, because $\Delta K_{oo} \rightarrow 0$ implies that $\kappa \rightarrow 0$, $N(\alpha) = 0$ in this case. In other words, this update formulation becomes exactly linear when all of the model DOF are measured.

To distinguish this approach from the previous one, the remainder of this paper will refer to the algorithm that performs a parameter correction based on minimizing Eq. (31) as the pseudoinverse formulation for flexibility error reduction algorithm (PseudoFLEX).

### Obtaining the Measured Flexibility Matrix from Dynamic Data

In Refs. 5–9, it is shown in detail how a measured flexibility matrix can be calculated from measured mass-normalized normal mode shapes, measured modal frequencies, and a rank-deficient estimate of the residual flexibility obtained from driving point measurements. The relationship can be expressed as

$$G^M = \Phi^M(\Lambda^M)^{-1}(\Phi^M)^T + \hat{G}_r^M \qquad (36)$$

where $\Phi^M$ is the measured mass-normalized modal matrix, $\Lambda^M$ is the diagonal matrix of the squares of the natural frequencies, and $\hat{G}_r^M$ is an estimate of the residual flexibility due to missing or out of bandwidth modes.

The referenced techniques outline a procedure for obtaining the quantities used in Eq. (36) in a systematic and practical manner. First, an overspecified state-space model is obtained from the measured frequency response data, using an efficient formulation of the eigensystem realization algorithm ERA called FastERA.[6] Next, the first-order damped realization is transformed to an equivalent second-order basis and the mass-normalized modal data are extracted. This is accomplished using the common basis-normalized structural identification algorithm.[5] The mass-normalization of the undamped measured modes is based on displacement compatibility at one or more driving point sensor locations. This initial modal model is then utilized in a frequency-domain curvefit procedure,[7] which yields an estimate of the measured mode shapes along with estimates for a residual flexibility and residual mass term. Using this residual flexibility term, the residual flexibility matrix can be formed using the methods outlined in Doebling et al.[8] and Doebling.[9]

It should be noted that the size of $G^M$ is only dependent on the number of measurement DOF, not the number of modes. Therefore, there is no penalty for including more modal information in the measurement. Also, because the flexibility matrix forms the basis of comparison in this approach, knowing the correspondence between measured and analytical mode shapes is unnecessary to perform the update. In addition, adding the estimate of the residual flexibility can reduce the effects of modal truncation when only a small number of modes are measured. This is demonstrated in the numerical example that follows.

## Numerical Simulation Results

### Kabe's Eight DOF Mass-Spring Model

These simulations were conducted using the eight DOF example presented by Kabe.[11] This model includes 8 masses and 14 springs with a connectivity as shown in Fig. 1. The model is characterized by large relative differences in stiffness, which lead to poor numerical conditioning and closely spaced modes.

Normalized sensitivity matrices for the 14 spring stiffness parameters were computed using Eq. (5). Table 1 contains two sets of spring stiffness values: the initial stiffness values, which are used to formulate the analytical model, and a set of perturbed spring stiffness values, which are used to generate simulated experimental data. It is assumed that the masses remain unchanged from their initial values of $m_1 = 0.001$, $m_2, \ldots, m_7 = 1.0$, and $m_8 = 0.002$. The mass and stiffness matrix of the experimental model are used to generate the complete set of experimental frequencies and mass-orthonormal mode shapes. The simulated data consist of an experimental modal set and an estimate of the residual flexibility matrix. The experimental modal set is taken to be a subset of this complete modal set, starting with the lowest frequency mode. The rest of the mode shapes and frequencies are considered to be unmeasured residual modes. To be consistent with experimental procedures, the estimate of the residual flexibility matrix is obtained using only the components of these residual modes that correspond to driving point sensor locations. To limit complexity, it is assumed that all of the sensor locations are also driving points. Using these simulated data, $G^M$ is formed using Eq. (36).

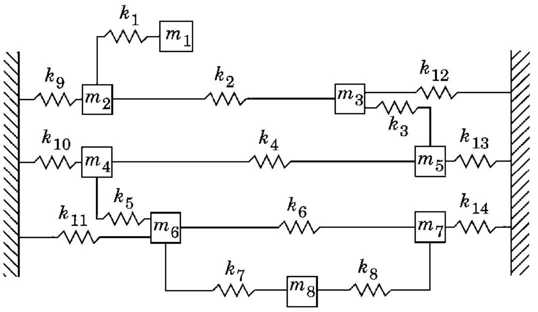


**Fig. 1 Eight DOF Kabe model.**

**Table 1 Kabe model stiffness parameters**

| Normalized parameter | Spring stiffness | Initial stiffness value | Perturbed stiffness value |
|---|---|---|---|
| $\alpha_1$ | $k_1$ | 1.5 | 2.0 |
| $\alpha_2$ | $k_2$ | 10.0 | 10.0 |
| $\alpha_3$ | $k_3$ | 100.0 | 200.0 |
| $\alpha_4$ | $k_4$ | 100.0 | 200.0 |
| $\alpha_5$ | $k_5$ | 100.0 | 200.0 |
| $\alpha_6$ | $k_6$ | 10.0 | 10.0 |
| $\alpha_7$ | $k_7$ | 2.0 | 4.0 |
| $\alpha_8$ | $k_8$ | 1.5 | 2.0 |
| $\alpha_9$ | $k_9$ | 1000.0 | 1500.0 |
| $\alpha_{10}$ | $k_{10}$ | 900.0 | 450.0 |
| $\alpha_{11}$ | $k_{11}$ | 1000.0 | 1500.0 |
| $\alpha_{12}$ | $k_{12}$ | 1000.0 | 1500.0 |
| $\alpha_{13}$ | $k_{13}$ | 900.0 | 450.0 |
| $\alpha_{14}$ | $k_{14}$ | 1000.0 | 1500.0 |

**Table 2 Normalized parameter value for FLEX update**

| Normalized parameter | Linear solution | Nonlinear solution | Exact solution |
|---|---|---|---|
| $\alpha_1$ | −0.33 | −0.25 | −0.25 |
| $\alpha_2$ | 0.22 | 0.00 | 0.00 |
| $\alpha_3$ | −0.70 | −0.50 | −0.50 |
| $\alpha_4$ | −0.22 | −0.50 | −0.50 |
| $\alpha_5$ | −0.66 | −0.50 | −0.50 |
| $\alpha_6$ | 0.41 | 0.00 | 0.00 |
| $\alpha_7$ | −0.92 | −0.50 | −0.50 |
| $\alpha_8$ | −0.29 | −0.25 | −0.25 |
| $\alpha_9$ | −0.50 | −0.33 | −0.33 |
| $\alpha_{10}$ | 0.76 | 1.00 | 1.00 |
| $\alpha_{11}$ | −0.53 | −0.33 | −0.33 |
| $\alpha_{12}$ | −0.53 | −0.33 | −0.33 |
| $\alpha_{13}$ | 0.78 | 1.00 | 1.00 |
| $\alpha_{14}$ | −0.50 | −0.33 | −0.33 |

### Updating all Spring Stiffnesses with Full-Order Flexibility Measurement

For these simulations, all 14 of the perturbed spring stiffness values are used to form the experimental model. It is assumed that perfect measurements are available at all eight DOF. Table 2 compares the linear, nonlinear, and exact solutions when the FLEX algorithm is used for this problem and all eight modes are used to form the measured flexibility matrix. Although the linear solution produces errors in the parameters, the nonlinear solution achieves an exact update. Additional simulations have shown that identical results are achieved using any number of modes with an estimate of the residual flexibility.

The next set of simulations was conducted using the PseudoFLEX algorithm. As discussed earlier, the update problem is exactly linear for the PseudoFLEX formulation, because the measurement and model DOF are the same in this case. Therefore, an iterative nonlinear solution is unnecessary. When there is no noise and all DOF are measured, an exact update of all 14 spring stiffnesses is again achieved using any number of measured modes and an estimate of the residual flexibility. When no residual flexibility estimate is used, five measured modes are needed to get an exact update. Without residual flexibility, this is the minimum number of modes necessary to uniquely determine the solution of the 14 parameters in this problem. Fewer modes would be needed if a smaller number of parameters are updated.

### Detecting Errors in Interior Elements with a Reduced-Order Measurement

Although the previous case illustrates that exact updates are achieved when all model DOF are measured, of greater interest is the ability of the algorithm to detect errors in interior elements using a reduced-order measurement. This is because the number of measurement DOF is typically much smaller than the number of

**Table 3 Normalized parameter values for reduced-order update of interior springs using one mode and a residual flexibility estimate**

| | Case 1 | | | Case 2 | | |
|---|---|---|---|---|---|---|
| Parameter | Linear solution | Nonlinear solution | Exact solution | Linear solution | Nonlinear solution | Exact solution |
| $\alpha_{10}$ | 0.00 | 0.00 | 0.0 | 0.55 | 1.00 | 1 |
| $\alpha_4$ | 0.58 | 0.50 | 0.5 | 0.12 | 0.50 | 0.5 |
| $\alpha_{13}$ | 0.00 | 0.00 | 0.0 | 0.55 | 1.00 | 1 |

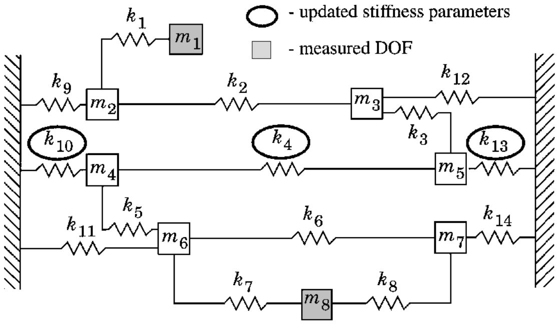


**Fig. 2 Measurement and model error locations for interior spring update.**

model DOF in applications of interest. For these simulations, it is assumed that only the two distant DOF associated with $m_1$ and $m_8$ are measured and the three most interior spring stiffnesses are to be updated. Figure 2 shows the location of the measurement DOF and the perturbed springs. Because only two DOF are measured, the experimental modal vectors contain only two elements. In other words, a $2 \times 2$ measured flexibility matrix is used to update the $8 \times 8$ analytical stiffness matrix in this example. For these simulations, only the PseudoFLEX results are presented. Similar results have also been achieved using the FLEX algorithm.

Two cases are examined. In the first, the interior model error is simulated by a 50% decrease in the spring stiffness associated with $\alpha_4$ (the spring between $m_4$ and $m_5$). For the second case, all three spring stiffnesses are changed. There is again a 50% decrease in the $\alpha_4$ spring, whereas the $\alpha_{10}$ and $\alpha_{14}$ springs have their stiffness increased by 100%. In both cases, only one measured mode along with a residual flexibility estimate is used for the update. In obtaining the residual flexibility matrix estimate, it is assumed that the sensor locations at $m_1$ and $m_8$ are driving point locations.

The results for both cases are shown in Table 3. In the first case, the linear solution was able to localize and reduce the parameter error from 50 to 16%. Starting with the values from the linear update, the nonlinear solution converges to the exact result in just a few iterations. In the second case, the linear solution produces substantial error in all three stiffness values. However, the nonlinear gradient search is again able to start with this linear solution and converge to the exact result in just a few iterations. These results demonstrate that it is possible to both localize and quantify model error involving relatively large parameter changes in a region located away from the measurement DOF. Even when the problem is nonlinear, the linear solution provides an initial parameter estimate that can be refined by a nonlinear search.

### Effect of Measurement Noise

An important consideration in the development of any model update algorithm is its sensitivity to uncertainty in the measurements. To study the effect of measurement noise, it is assumed that all modes are available and measurements are obtained at all DOF of the model. Measurement noise is simulated by adding white noise to each of the simulated measured mode shapes. The maximum magnitude of the noise vector coefficients is set to be the product of a noise percentage factor with the euclidean norm of the mass-normalized mode shape. The noise percentage factor remains the same for each of the modes.

The effect of measurement noise is studied by comparing the relative error in the updated stiffness values to the relative error in the mass-normalized measured modal matrix. The relative error in the updated stiffness values is expressed in terms of the normalized parameters as

$$\frac{\|\{p\}_{\text{final}} - \{p\}_{\text{exact}}\|}{\|\{p\}_{\text{exact}}\|} = \frac{\|\{\alpha\}_{\text{final}} - \{\alpha\}_{\text{exact}}\|}{\|\{1\} + \{\alpha\}_{\text{exact}}\|} \tag{37}$$

and the relative error in the mass-normalized modal matrix is given by

$$\frac{\|\Delta\Phi\|}{\|\Phi_{\text{exact}}\|} \tag{38}$$

where $\Delta\Phi$ is simply the matrix whose columns are the white noise vectors added to the individual mode shapes. For each algorithm, three update cases were studied. The first is the update of all 14 spring stiffness values. The second is the update of the three spring stiffness values with the most sensitivity in the error residual. The final case studied is the update of only the two parameters with the most sensitivity in the error residual. Several examples with varying amounts of measurement noise were generated for each test case. Figure 3 shows the results for simulations performed using the FLEX algorithm, and Fig. 4 shows the results using the PseudoFLEX algorithm.

The results demonstrate that sensitivity to measurement noise is a serious issue for both the FLEX and PseudoFLEX approaches when many parameters are estimated. With both approaches, virtually any

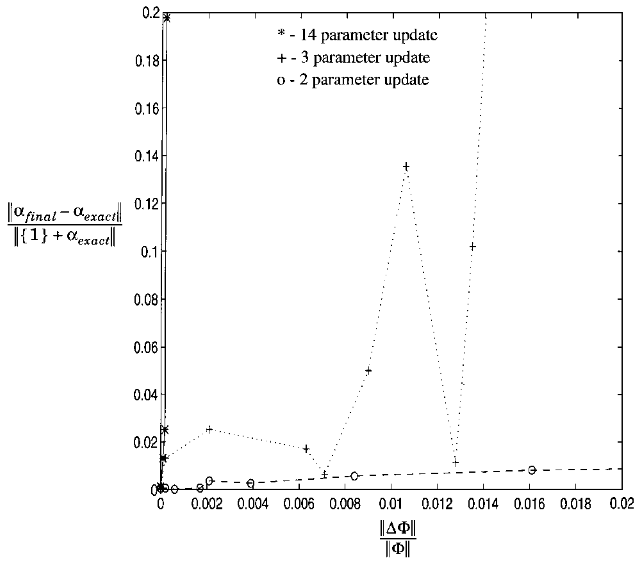


**Fig. 3 Effect of measurement noise on Kabe's problem using FLEX.**

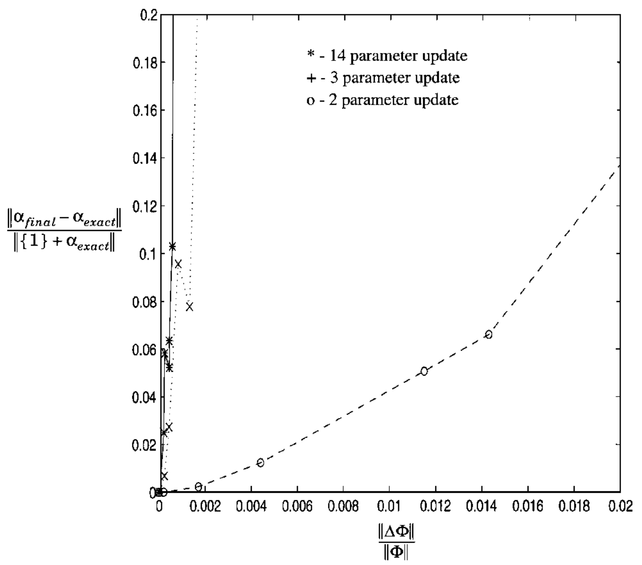


**Fig. 4 Effect of measurement noise on Kabe's problem using PseudoFLEX.**

amount of measurement noise caused substantial parameter errors in the 14 parameter updates. However, this error was typically concentrated in the parameters for which the error residual had little sensitivity. It should be noted that the full update of Kabe's problem is severely ill-conditioned, with the stiffness and mass values varying by over three orders of magnitude. Although this allows an update for the noise free case, it prevents an accurate estimate of all parameters in the presence of noise. In practice, parameters with virtually no sensitivity in the error would not be estimated. The results for the two and three parameter update cases demonstrate that the performance is improved as the problem becomes better conditioned. However, despite this improvement, the results show that measurement noise sensitivity is still significant, particularly for the PseudoFLEX algorithm, which magnifies errors even in the two parameter update case. On the other hand, the FLEX algorithm attenuates the error in the two parameter case. The effect of noise on PseudoFLEX, which deserves further investigation, is likely due to the fact that the resulting linear update equation has correlated noise on both the observation and the coefficient matrix. The least-squares solutions of overdetermined equations of this form are themselves research topics as discussed in Ref. 1.

## Experimental Application

This section presents results for updating a finite element model of a cantilever beam structure. Based on the simulation results of the previous section, the FLEX algorithm was chosen for this update. The dimensions and physical parameters for the beam are given in Table 4. An experimental modal analysis was conducted on this structure that yielded the first four bending modes. The identified modal frequencies are shown in Table 5. The beam was modeled by constructing a four-element finite element model. In addition to the elements used to model the beam, beam elements were added from each sensor location to its nearest beam node. This was done to account for the discrepancy between the actual sensor locations and the locations of the beam nodes. These beams were given a very high stiffness to make them appear as rigid links to the sensors. Also, point masses were added to the model to account for the additional mass of the sensors and cables. For the sake of comparison, the modal frequencies derived from this analytical model are also shown in Table 5. The objective in this problem is to use the experimental data and the FLEX algorithm to experimentally determine Young's modulus $E$ for the beam. Although simplistic, this affords us the luxury of determining a parameter that we already know with a high degree of confidence. To meet this objective, a measured static flexibility matrix is formed using the four experimentally determined mode shapes and frequencies and an estimate of residual flexibility obtained using the methods discussed previously. Using the full-order model, a normalized sensitivity matrix is computed with respect to $E$ for the beam. Young's modulus for the beam elements used to model the sensors is not updated.

**Table 4 Geometric and material parameters for cantilever beam structure**

| Parameter | Value |
|---|---|
| Length $L$, m | 1.5 |
| Width $b$, in. | 2.0 |
| Thickness $t$, in. | 0.5 |
| Young's modulus $E$, GPa | 70 |
| Density $\rho$, kg/m$^3$ | 2710 |
| Poisson's ratio $\nu$ | 0.346 |

**Table 5 Experimental and nominal analytical modal frequencies for cantilever beam**

| Mode description | Experimentally measured frequency, Hz | Analytical frequency, Hz |
|---|---|---|
| First bending | 4.34 | 4.26 |
| Second bending | 27.06 | 25.95 |
| Third bending | 77.55 | 76.63 |
| Fourth bending | 149.47 | 145.55 |

In this problem, there are only 13 measurement DOF, leading to a $13 \times 13$ measured flexibility matrix. By contrast, the full-order stiffness matrix being updated has 90 DOF. Also, because the sensor measurements are located at nodes offset from the beam, the model error being corrected is contained entirely in elements that do not touch measurement DOF.

Several updates were performed, starting with different values of $E$ in the nominal analytical model. These initial values are shown in Table 6 along with the resulting updated values for $E$. In each case, the update consistently converged to the same value, 84.3 GPa. Because the material is 6061-T6 aluminum, the actual value for $E$ should be around 70 GPa. The most likely explanation for this discrepancy is that the highly overdetermined set of equations given in Eq. (21) is leading to a large bias due to measurement noise. To help alleviate this effect, the number of observations contained in the right-hand side of Eq. (21) may be reduced. One way to accomplish this is to use only those observations corresponding to the largest elements of $G^M$, making sure that enough observations are included to uniquely determine the problem for the number of parameters updated. Using a reduced number of observations, the updates were again performed with the results again shown in Table 6. In the reduced-observation case, the parameter estimate converged to an improved value of $E = 76.87$ GPa. The remaining error could still be the result of measurement noise. Other explanations include errors in other model parameters or improper mass-normalization of the measured mode shapes. However, it is clear that the resulting update is reducing the error between the measured flexibility and the flexibility of the analytical model. Figure 5 shows

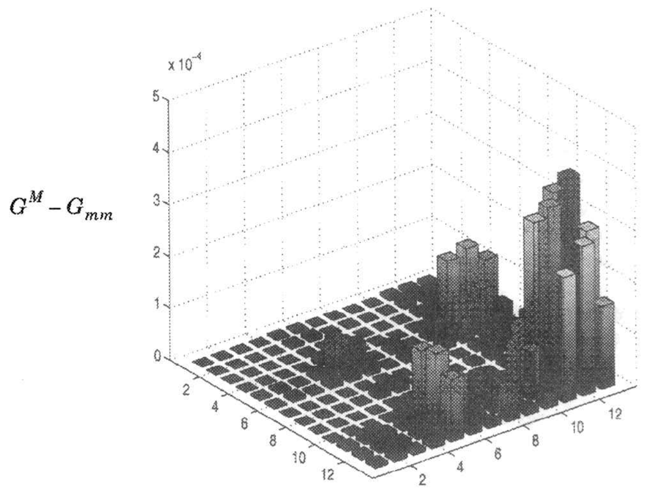


**Flexibility error for nominal model**

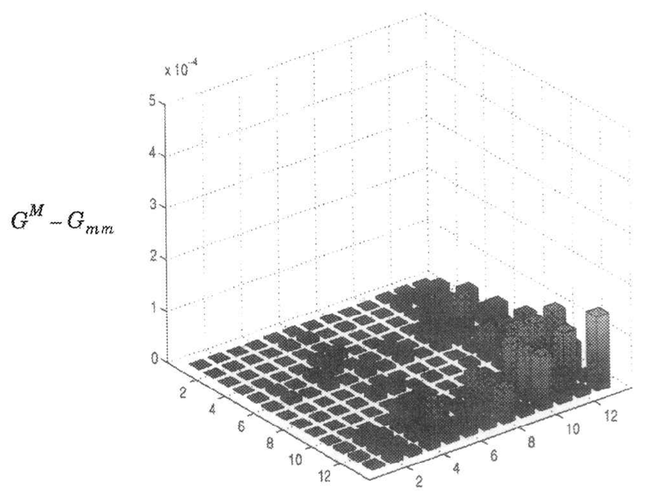


**Flexibility error for updated model**

**Fig. 5 Update reduces static flexibility error between model and measurement.**

**Table 6 Initial and updated values for Young's modulus**

| | Original update | | Update with reduced observations | | Nominal $E$ for T-6061 aluminum, GPa |
|---|---|---|---|---|---|
| Initial $E$, Gpa | $\alpha$ | Updated $E$, GPa | $\alpha$ | Updated $E$, GPa | |
| 7 | 11.05 | 84.33 | 9.98 | 76.87 | 70 |
| 35 | 1.41 | 84.33 | 1.20 | 76.87 | 70 |
| 70 | 0.20 | 84.33 | 0.10 | 76.87 | 70 |
| 84 | 0.00 | 84.33 | −0.08 | 76.87 | 70 |
| 105 | −0.20 | 84.33 | −0.27 | 76.87 | 70 |

the reduction in the flexibility matrix error residual achieved for the case where $E$ for the nominal model is 70 GPa.

## Conclusion

A new approach to model update has been presented that utilizes a measured static flexibility matrix obtained from dynamic testing. The measured flexibility matrix includes contributions from all the measured modes as well as any available residual flexibility information. By formulating the update problem in terms of static flexibility, the problem of modal correspondence between experiment and model is avoided. Also, choosing a small modal set to avoid excessive computations is unnecessary because the size of the flexibility matrix does not increase when additional modal information is added. In addition, the ability to easily incorporate residual flexibility reduces the effect of neglected residual dynamics due to modal truncation.

Simulation results show that the method can detect and quantify model errors that are deeply embedded in elements that do not touch the measurement DOF. The formulation allows the full-order analytical stiffness matrix to be updated, even when the measurement DOF are a small subset of the analytical DOF. The simulations also show that the algorithms are highly susceptible to measurement noise when the problem is ill-conditioned. This is particularly true of the PseudoFLEX algorithm, which showed a higher noise sensitivity than the FLEX algorithm.

Finally, experimental results for a cantilever beam structure demonstrate that the technique can be successfully applied to experimental data and that the effects of measurement noise are reduced by limiting the number of observations obtained from the flexibility error residual. The results show that the flexibility error between measurement and model are significantly reduced during the update.

## Acknowledgments

This research was sponsored by Sandia National Laboratories under Contract AJ-4223 and by the U.S. Department of Energy under Contract AC04-94AL85000. The authors would also like to acknowledge the Phillips Laboratory for its support through the U.S. Air Force Palace Knight program. The authors would like to specifically thank John Red-Horse of Sandia National Laboratories for giving his technical insights and suggestions throughout this work.

## References

[1]Friswell, M. I., and Mottershead, J. E., *Finite Element Model Updating in Structural Dynamics*, 1st ed., Kluwer Academic, Norwell, MA, 1995, pp. 86, 126–227.

[2]Lallement, G., Berriet, R., and Cogan, S., "Updating Finite Element Models Using Static Deformation," *Proceedings of the 10th International Modal Analysis Conference*, Society for Experimental Mechanics, San Diego, CA, 1992, pp. 494–499.

[3]Hajela, P., and Soeiro, F. J., "Structural Damage Detection Based on Static and Modal Analysis," *Proceedings of the 30th Structures, Structural Dynamics, and Materials Conference*, AIAA, Washington, DC, 1989, pp. 1172–1182 (AIAA Paper 89-1293).

[4]Sanayei, M., and Onipede, O., "Damage Detection in Structures Using Static Test Data," *AIAA Journal*, Vol. 29, No. 7, 1991, pp. 1174–1179.

[5]Alvin, K. F., and Park, K. C., "Second-Order Structural Identification Procedure via State-Space-Based System Identification," *AIAA Journal*, Vol. 32, No. 2, 1994, pp. 397–406.

[6]Peterson, L. D., "Efficient Computation of the Eigensystem Realization Algorithm," *Journal of Guidance, Control, and Dynamics*, Vol. 18, No. 3, 1995, pp. 395–403.

[7]Peterson, L. D., and Alvin, K. F., "A Time and Frequency Domain Procedure for Identification of Structural Dynamic Models," *Proceedings of the 35th Structures, Structural Dynamics, and Materials Conference*, AIAA, Washington, DC, 1994, pp. 14–24 (AIAA Paper 94-1731).

[8]Doebling, S. W., Alvin, K. F., and Peterson, L. D., "Measurement of Static Flexibility Matrices for Experiments with Incomplete Reciprocity," *Proceedings of the 36th Structures, Structural Dynamics, and Materials Conference*, AIAA, Washington, DC, 1995, pp. 2777–2791 (AIAA Paper 95-1090).

[9]Doebling, S. W., "Measurement of Structural Flexibility Matrices for Experiments with Incomplete Reciprocity," Ph.D. Dissertation, Dept. of Aerospace Engineering Sciences, Univ. of Colorado, Boulder, CO, May 1995.

[10]Guyan, R. J., "Reduction of Stiffness and Mass Matrices," *AIAA Journal*, Vol. 3, No. 2, 1965, p. 380.

[11]Kabe, A. M., "Stiffness Matrix Adjustment Using Mode Data," *AIAA Journal*, Vol. 23, No. 9, 1985, pp. 1431–1436.

[12]Lim, T. W., "A Submatrix Approach to Stiffness Matrix Correction Using Modal Test Data," *AIAA Journal*, Vol. 28, No. 6, 1990, pp. 1123–1130.

[13]Kailath, T., *Linear Systems*, Prentice–Hall, Englewood Cliffs, NJ, 1980, p. 656.

[14]Layton, J. B., "Multiobjective Control/Structure Design in the Presence of Practical Constraints," Ph.D. Dissertation, Dept. of Aerospace Engineering, Purdue Univ., Lafayette, IN, May 1992.

[15]Press, W. H., Flannery, B. P., Teukolsky, S. A., and Vetterling, W. T., *Numerical Recipes: The Art of Scientific Computing*, Cambridge Univ. Press, New York, 1986, pp. 307–312.

[16]Skelton, R. E., *Dynamic Systems Control: Linear Systems Analysis and Synthesis*, Wiley, New York, 1988, pp. 35–38.